A Band-Weighted Landuse Classification Method for Multispectral Images

Chunhong PAN, Gang WU, Veronique PRINET, Qing YANG, and Songde MA
National Lab of Pattern Recognition
Institute of Automation, Chinese Academy of Sciences, P. R. China
Email:*chpan@nlpr.ia.ac.cn*

Abstract

Landuse classification is an important problem in the remote sensing field. It can be used in a wide range of applications. In this paper, we propose a hybrid method fusing edges and regions information for the landuse classification of multispectral images. It mainly includes the steps of image pre-processing, initial segmentation and region merging. Especially, a novel spatial mean shift procedure is proposed so that some information can be extracted and used in the successive steps. Aiming at the multispectral images processing, we also design a band weighting strategy that give a proper weight to each band adaptively according to the region to be processed. Experimental results on the Landsat TM and ETM+ images validate the performance of the proposed method.

1. Introduction

Landuse (or landcover) classification, as an image labelling problem, plays an important role in the remote sensing field. This procedure assigns a ground cover label, such as water, urban, forest, crop, etc., to each image site based on the observed data at the site. In recent decades, many approaches to image segmentation or classification have been applied to landuse classification. According to the image site to be labelled, these approaches can be divided into four groups: the pixel-based methods, the boundary-based methods, the region-based methods and the hybrid methods [4, 8].

As for multispectral images classification, how to define a proper multispectral distance or how to assign proper weights to bands is an especially important issue worthy of considering because different bands present different spectral characteristics for different landcovers. Furthermore, even the regions under the same type of landcover may present rather different gray values in certain bands. Take the Landsat5 TM images as an example. In Figure 1, the two large water bodies, i.e. the lake in the image center and the river, appear different grays values in band 2 because the ability of water penetration is strong in this band and features underwater can therefore be reflected. On the contrary, they present similar gray values in band 4 due to the complete absorption by water. This indicates that band 4 is more helpful for water bodies recognition rather than band 2. Thus, it is necessary to properly select or weight bands for multispectral images classification. Several methods regard pixels as multivariate vectors and use the Euclidean distance to measure their homogeneity, which implicitly assumes that all bands contribute equally to the landcover response. This is obviously not true in most cases. The use of the Mahalanobis distance seems more reasonable but the estimation of the class-dependent covariance matrix usually requires a large number of training samples. Some PCA-based (Principle Component Analysis) and LDA-based (Linear Discriminant Analysis, i.e. Fisher's rule) band selection methods for multispectral or hyperspectral images were discussed in [7], but their objectives mainly lay in band decorrelation and data reduction. In these methods, the bands were selected globally according to statistic analysis of whole images (e.g. canonical analysis) but not adaptively to the landcover types of regions. Therefore, one of the most important motivations of this paper is to develop a region-adaptive method for band weighting.

In this paper, we present a hybrid landuse classification method for multispectral images. The image is first smoothed by the mean shift filter [5], and then an initial over-segmentation is carried out by means of seeded region growing. Thanks to the smoothing and the region-based segmentation, the salt-and-pepper noise and impure spectral noise are suppressed effectively. Moreover, an extension to the mean shift method, which we call spatial mean shift, is proposed in this paper. By the novel mean shift procedure, an assistant map can be created, from which homogeneous areas, edges and centers of small regions can be distinguished. Following the initial segmentation, a band-weighted EM clustering is then proposed for region merg-

(a) Band 1   (b) Band 2   (c) Band 3

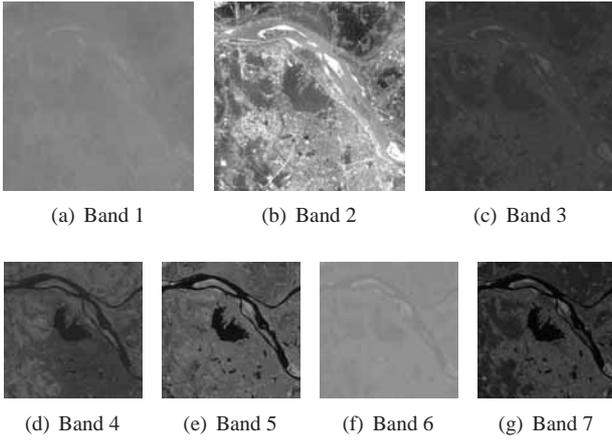(d) Band 4   (e) Band 5   (f) Band 6   (g) Band 7

Figure 1. Landsat5 TM images in Red River

ing. Especially, we design a band weighting strategy, and incorporate it to the EM algorithm. Here, the information of region boundaries and edges are fully used to determine the band weights, and such weighting strategy is adaptive to the region to be processed.

2. Mean shift procedure

The mean shift procedure [5] is essentially a detector for local maxima of a p.d.f. (probability density function) in a feature space. It can provide reliable solutions to many vision tasks, such as discontinuity preserving smoothing and image segmentaion. The choice of the mean shift filter for image smoothing here arises from the comparison research in [14], which reported that the mean shift filter had a good tradeoff between RSI (Relative Smoothing Index) and ERI (Edge Retention Index), compared with filters like Gaussian filter, median filter, bilateral filter, etc. An extension to the mean shift, which we call spatial mean shift, is proposed in this work. Some edges and regions information can be extracted from this novel mean shift prodedure, and thereafter used for both the initial segmentation and region merging. The principle of the mean shift is described in detail in the work of Comaniciu and Meer [5].

Before the mean shift smoothing, a PCA transformation is performed on the input multispectral images. It removes the correlation among bands and, furthermore, the transformed image may make evident features not discernable in the original data. Or alternatively, it may preserve the essential information content of the image [1]. In the case of the Landsat5 TM images, the transformed image only containing the first three components can preserve more than 95% of the essential information of the original seven-band image [2]. After this transformation, the input data are condensed into three channels and form a false color image. The successive operations, including the mean shift

smoothing and the initial segmentation, are performed on this false color image. This reduces the computational demands and improves the algorithm performance.

2.1. Image smoothing

For each image pixel $x_i, i = 1, 2, \cdots, M \times N$ (M and N is the number of image row and column, respectively), combining its spatial coordinate $x_i^s = (x_{i,row}, x_{i,column})$ with its corresponding range measurements $x_i^r = (x_{i,B_1}, x_{i,B_2}, \cdots, x_{i,B_d})$ (d is the number of bands), a joint spatial-range space can be constructed. Mean shift procedure can be generalized to this joint space, where the feature point is $x = (x^s, x^r)$, and the kernel function is $g_{s,r} = c \cdot g_s(\| \frac{x^s}{h_s} \|^2) g_r(\| \frac{x^r}{h_r} \|^2)$ with two bandwidth parameters h_s and h_r.

In our case, $d = 3$ for the PCA transformed false color image, while $d = 1$ for the single-band image. If g_s is defined as a uniform kernel

$$g_s(x) = \begin{cases} 1 & \text{if } \| x \| \leq 1 \\ 0 & \text{otherwise} \end{cases}$$

according to the principle [5], this is produced as

$$y_{j+1} = \frac{\sum_{x_i^s \in N(y_j^s, h_s)} x_i g_r(\| \frac{y_j^r - x_i^r}{h_r} \|^2)}{\sum_{x_i^s \in N(y_j^s, h_s)} g_r(\| \frac{y_j^r - x_i^r}{h_r} \|^2)} \tag{1}$$

where $N(y_j^s, h_s)$ is the neighborhood of y_j^s with radius h_s.

For each pixel $x = (x^s, x^r)$, initialize $y_1 = x$, compute y_j according to (1) until reaching the convergence point y_c, and replace the range component of x with y_c^r, and the filtered image will be obtained, where all pixels that converge to the same point have the same range values. Noises are suppressed effectively after smoothing, as illustrated in Figure 2.
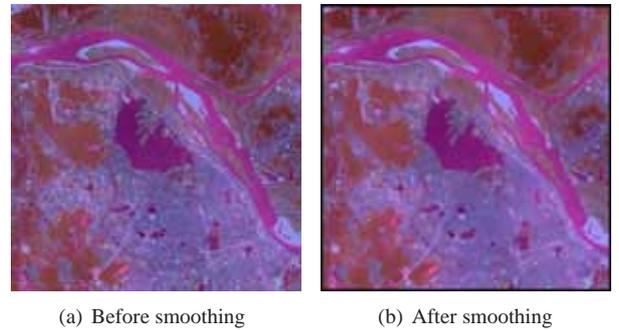

(a) Before smoothing   (b) After smoothing

Figure 2. PCA transformed false color image

2.2. Spatial mean shift

If we further consider the spatial location of the convergence point, something interesting is noted. Extracting the spatial component from (1), we have

$$y_{j+1}^s = \frac{\sum_{x_i^s \in N(y_j^s, h_s)} x_i^s g_r(\| \frac{y_j^r - x_i^r}{h_r} \|^2)}{\sum_{x_i^s \in N(y_j^s, h_s)} g_r(\| \frac{y_j^r - x_i^r}{h_r} \|^2)} \qquad (2)$$

It is a weighted mean of the spatial locations, called spatial mean shift. Let g_r be a Gaussian kernel. The above equation indicates that y_{j+1}^s tends to shift to areas where range values are homogeneous, but away from areas where edges exist. For each spatial location x^s, counting the number of points that converge to x^s, what we call spatial accumulation map can be produced. In this map, generally, value 0's occur along edges, where no point converges to, while 1's occur in the large homogeneous area because iteration (2) stops immediately by converging to y_1^s itself, and large values (say ≥ 5) occur in centers of small areas whose scale is less than h_s since most of points inside such a small area converge identically to its center. Thus, the edges, the small areas, and the large homogeneous areas can be discriminated according to the values of the accumulation map. Such information will be utilized in the successive steps.

Figure 3(a) shows the spatial accumulation map of the false color image. Enlarging the lake area in the center, it can be seen from Figure 3(b) that pixels are mostly 1's (the blue ones) within the lake area, and 0's (the white ones) along it. It indicates that a large homogeneous area exists within the lake, but edges along it. If we only consider the 0-value pixels, an edge map can be created. As depicted in Figure 4, the edge maps of different bands can be produced by applying the spatial mean shift procedure separately to each single-band image.
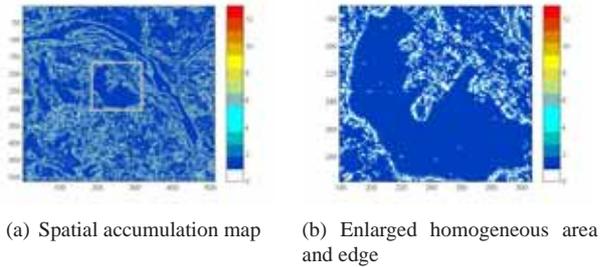

(a) Spatial accumulation map   (b) Enlarged homogeneous area and edge

Figure 3. Spatial accumulation map of the false color image

(a) Band 1   (b) Band 2   (c) Band 3

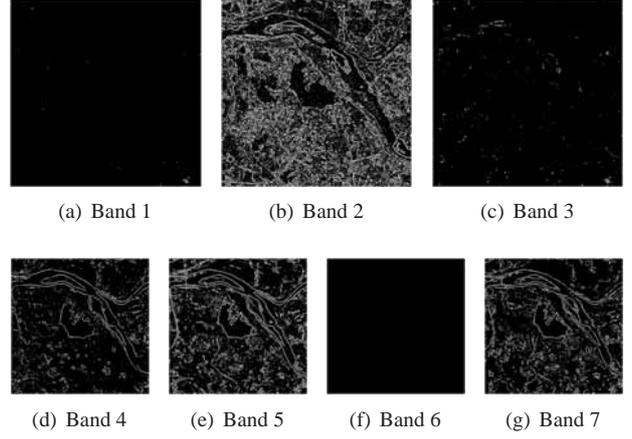(d) Band 4   (e) Band 5   (f) Band 6   (g) Band 7

Figure 4. Edge maps of each band

3 Initial segmentation by seeded region growing

Region growing involves two critical issues, the choice of seeds and the choice of growing criteria. Here, the seeds are selected according to the spatial accumulation map if either of the following conditions is satisfied.

(1) The point corresponds to a 1-value pixel and all of its neighbors (within a 3×3 window) are 1-value pixels as well;

(2) The point corresponds to a large-value pixel (say ≥ 5), and none of its neighbors (within a 3×3 window) is an edge pixel (i.e. ≥ 1).

These rules guarantee that the representatives of large homogeneous areas or the centers of small areas are selected as seeds. When a seed is selected, together with its neighbors within a 3×3 window, the initial region is determined and its mean and variance values are computed. Then the growing starts from the initial region. During this procedure, one would dynamically update the mean and variance of an already grown region R and compare them with a candidate pixel x in the neighborhood. Since channels of a PCA transformed image are uncorrelated to each other, the following inequalities can be tested separately

$$|pc_i(x) - \mu_i(R)| < k\sigma_i(R), \qquad i = 1, 2, 3 \qquad (3)$$

If they are all satisfied, pixel x will be included in region R. Here, pc_i is the ith component of the PCA transformed image and μ, σ are the current mean value and standard variance of region R. Suppose that the gray values in R follow the Gaussian distribution. The pixels passing the above test fall approximately within the central 86% range of gray values of R when $k = 1.5$ given. Figure 5 shows the initial segmentation and boundaries of the segmented regions.
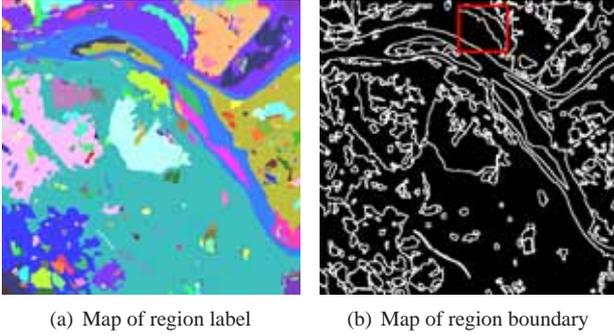
(a) Map of region label   (b) Map of region boundary

Figure 5. Initial segmentation results

4   Band-weighted region merging

In this section, the final classification will result from the initial over-segmentation by region merging. Here, the EM algorithm is used but, different from common applications, band weighting is incorporated in our classification task. As mentioned in Section 1, even the same type of landcover may present fairly different gray values in certain bands, which results in different colors in the PCA transformed false color image (see water bodies in Figure 2). Thus, the merging procedure is operated on each band of the original multispectral images instead of the PCA transformed one. Moreover, it is also expected that different bands contribute different weights. For instance, the two large water body regions (the lake and the river) in band 2 present quite different gray values, and their boundaries seem not so clear as the ones in bands 4, 5 and 7. Therefore, the weight of band 2 for water body region is supposed to be less than those in other bands.

Here, we determine the band weights by comparing the edge maps of each band with the boundary map of initially segmented regions. The basic idea is that, for a region in the initial segmentation map, if there exist remarkable edges along its boundary in certain bands, these bands will be considered as "good" bands for the said region, and will be assigned high weights. For example, consider Figure 4 and Figure 5(b), bands 4, 5, and 7 are good for water bodies because of their remarkable edges. It will be observed that our strategy of band weighting is adaptive for regions.

4.1. Estimation of band weight

The band weights are estimated by evaluating how "remarkable" an edge is relative to its corresponding region boundary. This problem is similar to the evaluation of edge detection. Both of them compare an edge map with a reference boundary map and check their matching cost. The related work was reviewed in [10]. Here, the CDM (Closest Distance Metric) algorithm [9] is adopted. For each pixel

	Band 1	Band 2	Band 3	
$W_i(R)$	0.0009	0.1875	0.0058	
	Band 4	Band 5	Band 6	Band 7
$W_i(R)$	0.2150	0.2793	0	0.2592

Table 1. Band weights of a water body area

of a region boundary (i.e. reference pixel), the edge map is inspected to find possible matchings within a previously defined searching window, such as a 5×5 window in our study that allows 2 pixels to be displaced. If there is no possible matching, the reference pixel is left unmatched. If it has multiple matchings, the edge pixel that is closest to the reference pixel is chosen. However, if its position as an edge pixel has already been chosen for a matching before, the next closest possible matching is selected. Therefore, the CDM criterion can build a one-to-one matching between the edge map and the reference map. The matching cost can be calculated in the following manner,

$$CDM(f,g) = \frac{Match(f,g)}{|f \cup g|} \qquad (4)$$

where f and g represent the edge map and the region boundary map, respectively. $Match(f,g)$ is the number of matched pixels. $|f \cup g|$ is the total number of pixels in f or g within the strip area that is the trace of the searching window moving along the region boundary. The weight of region R in the kth band is hereby denoted as $W_k(R) = CDM(f_k, g(R))$, where f_k is the edge map of the kth band, and $g(R)$ is the boundary map of region R. Moreover, for a region R, if the weights of all bands are very small, R is regarded as an invalid region and will be removed by merging it into the adjacent region with the most similar mean value, such as the red marked region in Figure 5.

The band weights of the lake region in the image center are listed as Table 1. Note that in bands 4, 5 and 7, the weights are much higher than those in other bands. This implies that these bands are more important for identifying water body region, and thereby demonstrates the feasibility of our approach to estimate band weights.

4.2   Region merging by band-weighted EM clustering

The EM algorithm is used here to merge regions into clusters. That is, the regions whose spectral measurements are close enough will be labelled as the same class. The EM [3, 12, 13] algorithm is a method for finding likeli-

hood parameter estimates when there are missing or incomplete data. Assume that a point $x_j, \quad j = 1, 2, \cdots, N$, in a d-dimensional feature space, is modelled as the K GMM (Gaussain Mixture Model) with the following probability density,

$$f(x|\Theta) = \sum_{i=1}^{K} \alpha_i f_i(x|\theta_i) \qquad (5)$$

$$f_i(x|\theta_i) = \frac{1}{(2\pi)^{d/2} det\Sigma_i^{1/2}} e^{-\frac{1}{2}(x-\mu_i)^T \Sigma_i^{-1}(x-\mu_i)} \qquad (6)$$

$$\sum_{i=1}^{K} \alpha_i = 1 \qquad (7)$$

where Θ represents the collection of parameters $(\alpha_1, \cdots, \alpha_K; \theta_1, \cdots, \theta_K)$, and θ_i represents μ_i and Σ_i. Given the initial parameters collection Θ, the updated equations take on the following form,

$$\alpha_i^{new} = \frac{1}{N} \sum_{j=1}^{N} p(i|x_j, \Theta^{old}) \qquad (8)$$

$$\mu_i^{new} = \frac{\sum_{j=1}^{N} x_j p(i|x_j, \Theta^{old})}{\sum_{j=1}^{N} p(i|x_j, \Theta^{old})} \qquad (9)$$

$$\Sigma_i^{new} = \frac{\sum_{j=1}^{N} p(i|x_j, \Theta^{old})(x_j - \mu_i^{new})(x_j - \mu_i^{new})^T}{\sum_{j=1}^{N} p(i|x_j, \Theta^{old})} \qquad (10)$$

$$p(i|x_j, \Theta) = \frac{\alpha_i f_i(x_j|\theta_i)}{\sum_{k=1}^{K} \alpha_k f_k(x_j|\theta_k)} \qquad (11)$$

until log likelihood

$$logL(\Theta|\chi) = log\Pi_{j=1}^{N} f(x_j|\Theta) \qquad (12)$$

increases by less than 1% from one iteration to the next.

In our case, the feature point x_j represents the mean value of region R_j in the initial segmentation map, and K is the number of predefined landuse classes (4 or 5 in common). Given the same initial parameters, the above computations are carried out on each band separately. When the iteration stops, each conditional probability $p(i|R_j, k)$, i.e. the chance that region R_j belongs to class $i(i = 1, \cdots, K)$ in band k, is achieved. Thanks to the total probability theorem, the chance that R_j entirely belongs to class i is,

$$p(i|R_j) = \sum_{k=1}^{M} p(k|R_j)p(i|R_j, k) \qquad (13)$$

where M is the number of bands (7 in our case), and the prior probability $p(k|R_j)$ is proportional to the band weight defined in formula (4):

$$p(k|R_j) = \frac{W_k(R_j)}{\sum_{k=1}^{M} W_k(R_j)} \qquad (14)$$

At last, the MAP (Maximum A Posteriori) criterion is used for class decision. For each region R_j, let it belong to the class that maximizes $p(i|R_j)$ for all i's. This classification results in the final landuse map.

Two issues are left to be solved in our EM-based region merging method, namely decisions of the class number K and the initial parameters μ^0 and Σ^0. Here, K is specified by users, and the initial parameters are obtained in the following manner. The first two regions are chosen from the initial segmentation map that have the largest distance, i.e. with the maximum difference of mean values. Then the third one is selected such that it has the largest sum of distances to the previous two regions. This goes on until the Kth region is found. This is in fact a greedy approach to find the K most different regions that maximizes the rule $J = min_{i,j} \sum_{i \neq j} \parallel \mu_i - \mu_j \parallel$, where μ_i and μ_j are mean value of the initial segmented regions, and within the sum symbol are $\sum_{k=1}^{K-1} k = K(K-2)/2$ terms of distances. As the K representatives of the initial segmented regions, the means and covariance matrices of the selected regions are regarded as the initial parameters.

5. Experimental results

The results demonstrated here utilize the Landsat5 TM images of the Red River area in Vietnam and the Landsat7 ETM+ images of the Jingjiang River area in China.

Figure 1 shows a sub-scene of the Red River area attained in April 2001. It contains seven bands, with a resolution of 30 meters and size of 512 by 512. In this scenario, there are obviously a lake in the center, and a river across the image. Other than water bodies, resident areas cover the bottom and right parts of the image, crop fields cover the left and top portions, and sand areas disperse near the water bodies.

Figure 6 shows a sub-scene of the Jingjiang area attained in September 2002 also with a size of 512 by 512. In addition to the TM bands, there is a panchromatic band with higher resolution of 15 meters for ETM+. Here, only bands 1-5 and 8 are used because they are of the same resolution of 30 meters. In this image, the dark areas in the center are water bodies. The top half part and the left-bottom part are mainly mountain frosts. The right-bottom part is mixed with crop fields and wet fields.

According to the above description, the classification procedure can be summarized as follows:

(a) Band 1   (b) Band 2   (c) Band 3

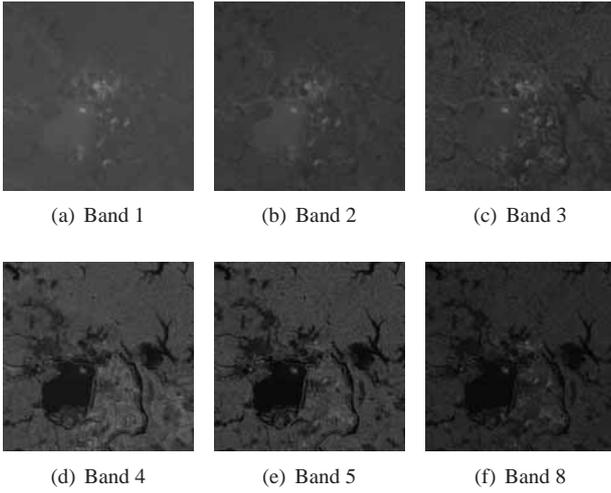(d) Band 4   (e) Band 5   (f) Band 8

Figure 6. Landsat ETM+ images in Jingjiang River area

1. Band reduction by the PCA transformation. Three first principle components are reserved containing more than 95% of the information of the original multispectral images;

2. Image smoothing and edge extraction by the mean shift procedure. The range window size h_r and the spatial window size h_s are 16 and 4, respectively;

3. Initial segmentation by seeded region growing. The coefficient $k = 1.5$ makes that the point passing the growing test fall within approximately 86% of the the central range of gray values of the grown region if under the condition of Gaussian distribution;

4. Region merging by band-weighted EM clustering. The class number K is given by users.

Both the Red River and the Jingjiang River images are classified into four classes and the final results are shown in Figure 7. Through prior knowledge, they correspond to the water body, resident area, crop field and sand area in the Red River image, and to the water body, crop field, mountain forest, and wet field patterns in the Jingjiang River image, respectively.

It is necessary to evaluate the classification result. According to the survey [11], the methods of empirical evaluation for image segmentation or classification fall into two groups: the discrepancy methods and the goodness methods. In the former category, some references or ground truths that present the expected results are first needed, and then the actual results are compared with the expected ones so as to count the discrepancy measures, such as correct accuracy, confusion matrix, Kappa analysis, etc. Different from the first category, the second methods measure results

directly by "goodness" parameters, such as intra-region uniformity, inter-region contrast, etc. Here, a goodness parameter (say the β index) is adopted to measure our results and compare with other methods. The β index is defined as the ratio of the total variation to with-class variation [6, 12],

$$\beta = \frac{\sum_{i=1}^{K} \sum_{j=1}^{n_i} (x_{ij} - \overline{X})^T (x_{ij} - \overline{X})}{\sum_{i=1}^{K} \sum_{j=1}^{n_i} (x_{ij} - \overline{X_i})^T (x_{ij} - \overline{X_i})} \qquad (15)$$

where K is the class number, n_i is the pixel number of the ith class; X_{ij} is the jth pixel value in class i, $\overline{X_i}$, $\overline{X}$ are mean values of the ith class and the total image, respectively. For a M band multispectral images, they are all M-dimensional vectors. β indicates the homogeneity of the classification result. For a given image and K value, the higher the homogeneity within the classified regions is, the higher the β index will be. β also increases with the class number K. In general, a high β value implies a good classification result.

Here, the class number K is given by users. From the plots of β versus K illustrated in Figure 8, it can be observed that $K = 4$ is reasonable, as the points where $K = 4$ are the corners of the curves. In other word, the increase of β becomes slow when $K > 4$.

In order to demonstrate the performance of the proposed method, comparisons are made with two common methods, the EM and FCM algorithms, without band weighting. For those methods, the preprocessing and the initial segmentation are the same, but in the region merging step, the EM or FCM (Fuzzy C-Mean) algorithm are directly implemented on the M-band multispectral images, and the feature points are M-dimensional vectors. Table 2 lists the comparison results. It indicates that the proposed band-weighted EM method is much better than the common EM method without band weighting, and slightly better than the FCM method in terms of the β index. These comparisons demonstrate the advantage of the proposed method against the method without band weighting.

6 Conclusions and Discussions

In this paper, a novel unsupervised landuse classification method for multispectral images is proposed. Its novelty lies in two aspects. First, we extend the mean shift procedure to the spatial space and, from the spatial mean shift procedure, some useful information can be extracted for successive operations, such as seeds selection in initial segmentation and band weighting in region merging. Second, a band weighting strategy is presented. The edge information obtained from the spatial mean shift procedure and the region boundary information obtained from the initial segmentation is used to evaluate the region-adaptive weights of each band. Experiments show that with the same initial

	FCM	EM	Band-weighted EM
Red River	1.99	1.26	2.09
Jingjiang River	2.04	1.36	2.16

Table 2. Methods comparison

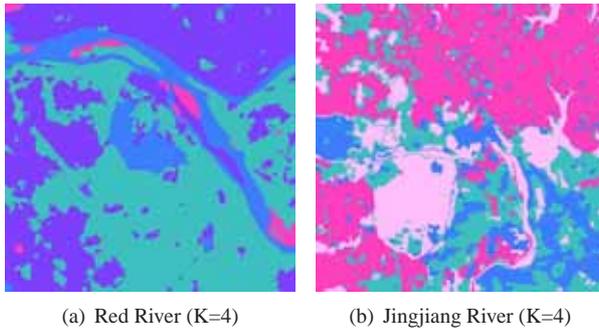conditions, the proposed method is superior to the method without band weighting under the measure of the β index.

(a) Red River (K=4) (b) Jingjiang River (K=4)

Figure 7. Final classification
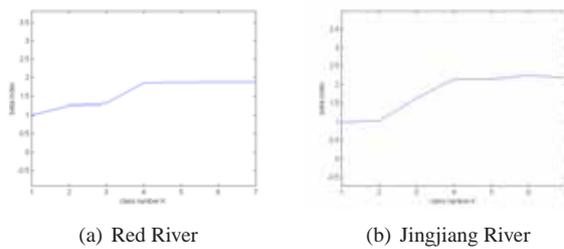

(a) Red River (b) Jingjiang River

Figure 8. Curves of the index β against class number K

References

[1] John A. Richards and Xiuping Jia, Remote Sensing Digital Image Analysis: An Introduction, (3rd Edition), Springer, 1999.

[2] Yingshi Zhao, Principles and Methods for Remote Sensing Application and Analysis, Beijing: Science Press, 2003.

[3] Sergios Theodoridis and Konstantinos Koutroumbas, Pattern Recognition, (2nd Edition), Amsterdam; Boston: Academic Press, 2003.

[4] Carolyn Evans, et al, "Segmentation Multispectral Landsat TM Images into Fiel Units", IEEE Trans. Geoscience and Remote Sensing, vol. 40, no. 5, pp. 1054-1064, May 2002.

[5] Dorin Comaniciu and Peter Meer, "Mean Shift: A Robust Approach Toward Feature Space Analysis", IEEE Trans. Pattern Analysis and Machine Intelligence, vol. 24, no. 5, May 2002.

[6] S. K. Pal, A. Ghost, and B. Uma Shankar, "Segmentation of remotely sensed images with fuzzy thresholding, and quantitative evaluation", Int. J. Remote Sensing, vol. 21, no. 11, pp. 2269-2300, Nov 2000.

[7] Agustin Ifarraguerri and Michael W. Prairie, "Visual Method for Spectral Band Selection", IEEE Geoscience and Remote Sensing Letters, vol. 1, no. 2, pp. 101-106, Apr 2004.

[8] C. A. Shah, et al, "Some Recent Results on Hyperspectral Image Classification", web.syr.edu/ pwatanac/IEEE-GRS2003.pdf, 2003.

[9] Tsolmongerel Orkhonselenge, "Texture based segmentation of remotely sensed imagery for identification of geological units", Master Thesis of ITC (International Institute for Geo-Information Science and Earth Observation, Netherlands), www.itc.nl/ library/Papers-2004/msc/gfm/tsolmongerel.pdf, Feb 2004.

[10] Miguel Segui Prieto and Alastair R. Allen, "A Similarity Metric for Edge Images", IEEE Trans. Pattern Analysis and Machine Intelligence, vol. 25, no. 10, pp. 1265-1273, Oct 2003.

[11] Y. J. Zhang, "A survey on evaluation methods for image segmentation", Pattern Recognition, vol. 29, no. 8, pp. 1335-1346, 1996.

[12] Sankar K. Pal and Pabitra Mitra, "Multispectral Image Segmentation Using the Rough-Set-Initialized EM Algorithm", IEEE Trans. Geoscience and Remote Sensing, vol. 40, no. 11, pp. 2495-2501, Nov 2002.

[13] Chad Carson, et al, "Blobworld: Image Segmentation Using Expectation-Maximization and Its Application to Image Querying", IEEE Trans. Pattern Analysis and Machine Intelligence, vol. 24, no. 8, pp. 1026-1038, Aug 2002.

[14] Zhaohui Zhang, "Study on Automatic Registration of Multi-Sensor Satellite Images", Ph.D. Dissertation of Ntaional Laboratory of Pattern Recogntion, Institute of Automation, Chinese Academy of Sciences, 2003.